# Ultrasound Imaging and Image Segmentation in the area of Ultrasound: A Review

[1]Kalpana Saini, [2]M.L.Dewal, [3]Manojkumar Rohit
*[1]Research Scholar, Deptt. of Electrical Engg.,IIT Roorkee, India*
*[2]Assistant professor, Deptt. of Electrical Engg.,IIT Roorkee, India*
*[3]Associate Professor, Deptt. of Cardiology, PGIMER Chandigarh, India*
*[1]kal_2312@rediffmail.com, [2]mohanfee@iitr.ernet.in, [3]manoj_786@hotmail.com*

***Abstract***

*Segmentation remains a necessary step in medical imaging to obtain qualitative measurements such as the location of objects of interest as well as for quantitative measurements such as area, volume or the analysis of dynamic behavior of anatomical structures over time. Among these images, ultrasound images play a crucial role, because they can be produced at video-rate and therefore allow a dynamic analysis of moving structures. Moreover, the acquisition of these images is non-invasive, cheap, and does not require ionizing radiations compared to other medical imaging techniques. On the other hand, the automatic segmentation of anatomical structures in ultrasound imagery is a real challenge due to acoustic interferences (speckle noise) and artifacts which are inherent in these images. Here we discuss the ultrasound image segmentation methods, in a broad sense, focusing on techniques developed for medical. First, we present basic methods of image segmentation and forming of ultrasound images. After that we discuss the basics on ultrasound image segmentation. Second section explains the ultrasonic image segmentation methods based on clinical applications. On the other hand Third section explains the ultrasound image segmentation based on particular methodology.*

***Keywords:*** *Segmentation; Ultrasound; Speckle Noise; Artifacts; ionizing radiations*

## 1. Introduction

Image analysis usually refers to processing of images by computer with the goal of finding what objects are presented in the image. Image segmentation is one of the most critical tasks in automatic image analysis.

In a standard ultrasound system there are three basic types of data available for analysis: radiofrequency (RF) signals, envelope-detected signals, and B-mode images. A transmit/receive ultrasound transducer receives multiple analogue radio-frequency (RF) signals which are converted to digital RF signals and beam formed into a single RF signal. The RF signal is then filtered, and envelope detection is performed to give an envelope-detected signal. Finally, the envelope-detected signal undergoes log compression, and often proprietary post-processing is applied to give a grayscale representation. The resulting signals are then interpolated and rasterized to give a B-mode or display image [1].

## 2. Different Methods of Image Segmentation

Segmentation Algorithms mainly based on two basic properties:

1. *Discontinuity (Edge based Approaches)* : Based on abrupt change in Intensity

2. *Similarity(Region based Approaches )* : Similar according to predefined Criterion

### 2.1 Edge Based Approaches

Edge detection is a well-developed field on its own within image processing. Region boundaries and edges are closely related, since there is often a sharp adjustment in intensity at the region boundaries. Edge detection techniques have therefore been used as the base of another segmentation technique.

### 2.2 Similarity

#### 2.2.1 Thresholding

Segmentation problems requiring multiple thresholds are best solved using region growing methods. Thresholding can be viewed as:

T = T[x, y, p(x, y), f(x, y)]

Where f(x, y) is gray-level at (x, y) and p(x, y) denotes some local property, for example average gray level in neighborhood.

A thresholded image g(x, y) is defined as

$$g(x, y)=\begin{cases}1, f(x, y) > T \\ 0, f(x, y) < T\end{cases}$$

where 1 is object and 0 is background

When T = T[ f(x, y) ], threshold is global
When T = T[ p(x, y), f(x, y) ], threshold is local
When T = T[ x, y, p(x, y), f(x, y) ], threshold is dynamic

#### 2.2.2 Region-Based Segmentation

Basic formulation
Let R represent the entire image region
The segmentation process partitions R into n subregions, R1,
R2, . . . , Rn, such that...

(a) $\bigcup_{i=1}^{n} R_i = R$

(b) $R_i$ is a connected region, i = 1, 2, . . . , n

(c) $R_i \bigcap R_j = \phi$ for all i and j, i 6= j

(d) $p(R_i)$ TRUE for i = 1, 2, . . . , n

(e) $P\left(R_i \bigcup R_j\right)$ = FALSE for i 6= j

Here $P(R_i)$ is logical predicate defined over all points in $R_j$
(a) Every pixel must be in a region
(b) All the points in a region must be “connected”
(c) Regions must be disjoint
(d) For example $P(R_i)$ = TRUE if all the pixels in $R_i$ have the same gray level
(e) Regions $R_i$ and $R_j$ are different in some sense

**Region growing**

• Start from a set of seed points and from these points grow the regions by appending to each seed those neighboring pixels that have similar properties
• The selection of the seed points depends on the problem. When a priory information is not available, clustering techniques can be used: compute the above mentioned properties at every pixel and use the centroids of clusters
• The selection of similarity criteria depends on the problem under consideration and the type of image data that is available
• Descriptors must be used in conjunction with connectivity (adjacency) information
• Formulation of a "stopping rule". Growing a region should stop when no more pixels satisfy the criteria for inclusion in that region.
• When a model of the expected results is partially available, the consideration of additional criteria like the size of the region, the likeliness between a candidate pixel and the pixels grown so far, and the shape of the region can improve the performance of the algorithm.

**Region splitting and merging**

Subdivide an image initially into a set of arbitrary, disjoint regions and then merge and/or split the regions in an attempt to satisfy the necessary conditions
Let R represent entire image region and select a predicate P
(1) Split into four disjoint quadrants any region $R_i$ for which

$$p(R_i) = \text{FALSE}$$

(2) Merge any adjacent regions $R_j$ and $R_k$ for which

$$P\left(R_i \bigcup R_k\right) = \text{FALSE}$$

(3) Stop when no further merging or splitting is possible

**Split and merge**

Define $p(R_i)$ = TRUE if at least 80% of the pixels in $R_i$ have the property $|z_i - m_i| < 2\sigma_i$

If $p(R_i)$ = TRUE the value of all the pixels in $R_i$ are set equal to mi

Splitting and merging are done using the algorithm on the previous transparency
Properties based on mean and standard deviation attempt to quantify the texture of a region
Texture segmentation is based on using measures of texture for the predicates $P(R_i)$.

Segmentation algorithms have had fairly limited application in ultrasound imaging. High levels of speckling present in ultrasound images make accurate segmentations difficult. Furthermore, the real-time acquisition in ultrasound makes it better suited for motion estimation tasks ([3, 4]) where active contours, because of their dynamic nature, are often used. Ultrasound is also often employed in detecting pathology using textural classifiers [5] but regions of interest are typically obtained through manual interaction.

Nevertheless, some automated segmentation work has been performed in ultrasound for extracting a variety of structures. In [6], a thresholding of intensity and texture statistics was used to segment ovarian cysts. Deformable models have had good success in ultrasound applications such as in the segmentation of echocardiograms [7, 8, 9]. In [10], an active contour was used to determine the boundary of the calcaneus in broadband ultrasonic attenuation parameter images, which are less noisy than standard ultrasound images. In [12], deformable models were used to determine the boundary of the fetus and the fetus head respectively. Deformable models have also been used to segment cysts in ultrasound breast images [14]. Other methods have been applied for the segmentation of coronary arteries in

intravascular ultrasound images [13] and for segmenting the pubic arch in transrectal ultrasound [11].

## 3. Classification of Ultrasound Segmentation based on Clinical Application

### 3.1 Echocardiography

Echocardiography is the application of ultrasound for imaging of the heart. Standard ultrasound techniques are used to image two-dimensional slices of the heart. Apart from 2-D, conventional echocardiography also employs M-mode and Doppler. Color Doppler is used to image flowing blood. Continuous wave Doppler and Pulsed wave Doppler are used to measure the velocity of flowing blood

The quality of data, and hence challenges for segmentation, vary depending on the view due to the anisotropy of ultrasound image acquisition, artifacts such as shadowing from the lungs, and attenuation which can be strong. Segmentation methods should also have strategies for avoiding the papillary muscles. Reliably finding the outer wall (often called Epicardial border detection) is much more challenging, particularly from apical views. There are many papers on left ventricle tracking which deal with the tracking/deformation model independent of feature extraction or the imaging modality. Three-dimensional echocardiography facilitates spatial recognition of intracardiac structures, potentially enhancing diagnostic confidence of conventional echocardiography. Three-dimensional echocardiography requires the collection of a volumetric data set where each image (cut plane) is defined with respect to its exact position in space. Early work used either freehand ultrasound (with 2-D image acquisition synchronized with recording the location of the slice with a position sensor), rotational 3- D probes which acquired a sparse set of 2-D image sequences, or real-time 3-D echocardiography based on the Volumetric system [17], [18].

Mishra *et al.* [19] proposed an active contour solution where the optimization was performed using a genetic algorithm. In a first image, the preprocessed contour after low pass filtering and morphological operations is optimized using GA for rough boundary delineation at fixed number of sample points were used to define an initial estimate of the contour. A nonlinear mapping of the intensity gradient was used in the energy functional which is minimized. The final contour was used to initialize contour finding in the next time frame. Mignotte and Meunier [20] choose to use a statistical external energy in a discrete active contour for the segmentation of short axis parasternal images, arguing that this was well-suited in ultrasound images with significant noise and missing boundaries. To this end, a shifted Rayleigh distribution was used to model gray levels statistics.

Level sets are often considered as an alternative to active contours and this approach has also been considered for echocardiographic image segmentation. Yan [21] considered applying the level set method to echocardiographic images using an adaptation of the fast marching method. To reduce errors attributed to using local feature (intensity gradient) measurements, they used an average intensity gradient-based measure in the speed term. The method was applied to a parasternal short axis and an apical four-chamber view sequence but the results were only discussed qualitatively.

### 3.2 Breast

Breast cancer occurs to over 8% women during their lifetime, and is a leading cause of death among women. Sonography is superior to mammography in its ability to detect focal abnormalities in the dense breasts and has no side-effect.

Since the underlying molecular mechanism of this disease still remains unknown, early detection and diagnosis are very essential in reducing the mortality. More and more emphases are on early detection and diagnosis of breast cancer. Currently, breast ultrasound (BUS) imaging is a valuable method in early detection and classification of breast lesions [22]. Sonography was more effective for women younger than 35 years old of age. The results [17] show that the denser the breast parenchyma, the higher the detection accuracy of malignant tumors using US. The accuracy rate of breast ultrasound imaging has been reported to be 96-100% in the diagnosis of simple benign cysts [18]. It has been shown that breast sonography is superior to the mammography in detecting focal abnormalities in the dense breasts of adolescent women [24]. Furthermore, sonography can display mass obscured mammgraphically by dense tissue, and it is low cost, portable and has no ionizing radiation [25].

Thus, the principal segmentation challenges pertain to characterizing the textured appearance and geometry of a cancer relative to normal tissue, and accommodating artifacts such as the possibly strong attenuation across an image and shadowing, as well as the "fuzziness" of cancerous mass boundaries which makes border delineation difficult. Importantly, as we see below, the studies of Stavos [26]–[28] have greatly influenced the design of algorithms for breast mass detection. Interestingly, no significant work has looked at the screening case, i.e., most work has assumed the presence of a, typically single, suspicious mass.

Horsch [29] presented a method involving thresholding a preprocessed image that has enhanced mass structures. Comparison is made of a partially automatic and fully automatic version of the method with manual delineation on 400 cases/757 images (124 "complex" cysts, 182 benign masses, and 94 malignant masses). They compute four image-based features (shape, echogeneity, margin, and posterior acoustic behavior) defined respectively in terms of the depth-to-width ratio, autocorrelation, "normalized radial gradient," and comparison of gray levels, to test their effectiveness at distinguishing malignant and benign masses.

Neural network (NN) based methods have proved to be popular in this area. These aim to make a classification decision based on a set of input features. For instance, Chen *et al.* [30] presented a NN approach where input features were variance contrast, autocorrelation contrast, and the distribution distortion in the (Daubechies) wavelet coefficients and an multilayered perceptron neural (MLP) network with one hidden layer was trained by error backpropagation.

Xiao [31] presented an expectation-maximization method that simultaneously estimates the attenuation field at the same time as classification of regions into different (intensity-based) regions. The number of regions (classes) needs to be specified, which in the intended application is not a strong limitation. That method was tested on experimental data with different time gain compensation (TGC) settings to show that their approach gave consistent segmentations under different TGC settings but has not undergone a large clinical assessment. This method is compared to that of Boukerroui in [32]. Madabhushi and Metaxas [33] combined intensity, texture information, and empirical domain knowledge used by radiologists with a deformable shape model in an attempt to limit the effects of shadowing

and false positives. Their method requires training but in the small database . Using manual delineation of the mass by a radiologist as a reference, and the Hausdorff distance and average distance as boundary error metrics, they showed that their method is independent of the number of training samples, shows good reproducibility with respect to parameters, and gives a true positive area of 74.7%. They also argued that it has automation advantages over the work of Horsch [29].

Sahiner [34] compared 2-D and 3-D intensity-gradient active contour segmentation based methods, the active contour initialized by hand, and with algorithm parameters determined empirically.

### 3.3 Prostate

Prostate diseases are very common in adult and elderly men, and prostate boundary detection from ultrasonographic images plays a key role in prostate disease diagnosis and treatment. However, because of the poor quality of ultrasonographic images, prostate boundary detection still remains a challenging task. Currently, this task is performed manually, which is arduous and heavily user dependent. To improve the efficiency by automating the boundary detection process, numerous methods have been proposed.

One of the most common imaging modalities that is used to visualize prostate for the purpose of diagnosis and biopsy is TRUS. Although currently, boundary of prostate images are mainly manually outlined on TRUS images by experienced radiologists, however due to poor contrast of these images, missing boundary segmentations, shadows and echo dropouts, the segmentation results are very subjective and vary between different radiologists. In general, prostate boundaries are routinely outlined in transverse parallel 2-D slices along the length of the prostate. This has led to the development of a number of methods for (semi-) automatic detection of prostate boundaries.2. An example of prostate segmentation from Gong [35] is shown in Fig. 1.

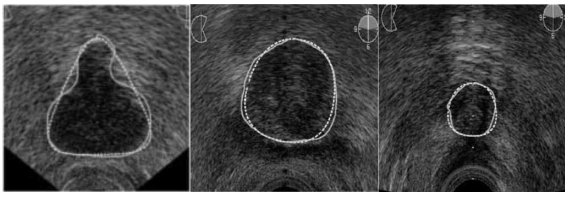

**Figure 1**. Segmentation example of transverse ultrasound images of the prostate from Gong *et al* [35]; the solid contours are the ground truth established by averaging five experts' manual outlining and the dotted contour are the computer generated boundaries.

Recent work has focused on incorporating prior information about shape and speckle models. For instance, Knoll [36] proposed employing a parametrization of a snake based on a 1-D dyadic wavelet transform as a multiscale boundary curve analysis tool. The initialization of the snake used template matching between contour models of a training set and significant image edges.

Abolmaesumi and Sirouspour [37] developed a 2-D boundary extraction method based on a probabilistic data association filter. They posed the 2-D segmentation problem as an estimation of a moving object along the cavity boundary, where the motion is governed by a finite set of dynamical models subject to uncertainty. Hence, the motion model along the

contour models the prior smoothness of the contour. Angular discretisation of the contour from a manually selected seed point inside the cavity was used to estimate the radial distance of the boundary points to the seed point.

Yu [38] presented a two-step semi-automatic active contour based segmentation method. First, an initial elliptical approximation of the contour was obtained using two manually selected points. A rough binary segmentation was then obtained by optimizing an area-weighted mean-difference criterion in a level sets framework. Finally, a finer segmentation was accomplished via a parametric active contour model in a polar coordinate system. In the second stage, a speckle reducing anisotropic diffusion, (SRAD) [39], was applied to enhance the images and the instantaneous coefficient of variation (ICOV) was utilized as an edge cue in the derivation of the external energy of the active contour model. Note that log-compressed -scan images have to be decompressed before applying the SRAD algorithm. It is reported in [39] and [40] that the ICOV allows for balanced and well-localized edge strength measurements in bright as well as in dark regions of speckle images.

### 3.4 Vascular Disease

Intravascular ultrasound (IVUS) is a catheter based medical imaging technique particularly useful for studying atherosclerotic disease. It produces cross-sectional images of blood vessels that provide quantitative assessment of the vascular wall, information about the nature of atherosclerotic lesions as well as plaque shape and size. Automatic processing of large IVUS data sets represents an important challenge due to ultrasound speckle, catheter artifacts or calcification shadows. A new three-dimensional (3-D) IVUS segmentation model, which is based on the fast-marching method and uses gray level probability density functions (PDFs) of the vessel wall structures, was developed. The gray level distribution of the whole IVUS pullback was modeled with a mixture of Rayleigh PDFs. With multiple interface fast-marching segmentation, the lumen, intima plus plaque structure, and media layers of the vessel wall were computed simultaneously. The PDF-based fast-marching was applied to 9 *in vivo* IVUS pullbacks of superficial femoral arteries and to a simulated IVUS pullback. Accurate results were obtained on simulated data with average point to point distances between detected vessel wall borders and ground truth 0.072 mm.

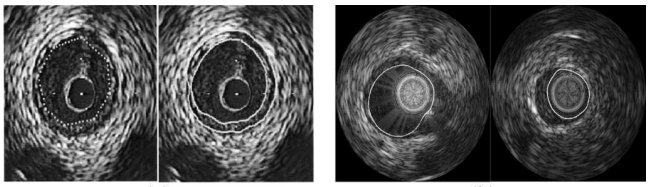


**Figure 2.** Segmentation example of IVUS images (vascular disease). (a) Example taken form Klingensmith *et al.* [48] showing the initial contour and the final borders. (b) Two segmentation examples of the automatic algorithm by Brusseau *et al.* [49].

On *in vivo* IVUS, a good overall performance was obtained with average distance between segmentation results and manually traced contours 0.16 mm. Moreover, the worst point to point variation between detected and manually traced contours stayed low with Hausdorff distances 0.40 mm, indicating a good performance in regions lacking information or

containing artifacts. In conclusion, segmentation results demonstrated the potential of gray level PDF and fast-marching methods in 3-D IVUS image processing [45].

Sonka [46] presented a semi-automatic knowledge based segmentation approach that identifies the internal and external lumina and the plaque–lumen boundaries. A novelty of the approach was the attempt to incorporate knowledge to mimic constraints used by an experienced ultrasonographer. The method used dynamic programming to solve a cost function based on edge strength and incorporated *a priori* knowledge about cross-sectional arterial anatomy (such as object shape, edge direction, double echo pattern, wall thickness). However, the method has several modeling limitations namely: the edge strength did not include speckle statistics and some prior information was included in a binary fashion with hard thresholds. An extension of the DDC (Discrete Dynamic Contour) model has been proposed for 3-D semi-automatic segmentation of the lumen and adventitial borders in serial IVUS images [47].The same group presented a faster method,

The fast active surface (FAS) [48] based on Williams and Shah's fast active contours (see Fig. 2a) for an example result). The former method is a force acceleration technique and the latter is a neighborhood-search method, and both snakes used only intensity gradient information. An editing tool was provided for user correction. In experiments, both techniques performed well although the FAS was 60 times faster.

The above methods use simple derivative operators to estimate intensity gradients. Recently Pardo *et al.* [50], proposed a statistical deformable model that was applied to IVUS images. They used a bank of Gaussian derivative filters, at different orientations and scales, to locally describe edge/non-edge cues, in an adaptive fashion (i.e., locally). The feature space was reduced by linear discriminate analysis, and a parametric classifier was employed to guide the model deformation by minimizing the dissimilarity between measured image features and the learned ones. The statistical learning approach made the algorithm more robust in comparison to using intensity gradient information, which supposes a prior model of the edge.

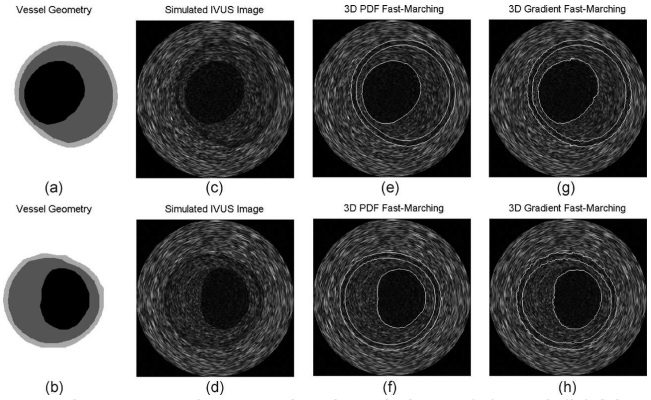


**Figure 3 .**Segmentation examples on simulated data. (a) and (b) Vessel geometries and (c) and (d) simulated IVUS cross-sectional images. Lumen, thickened intima, and media detected boundaries with (e) and (f) PDFs and (g) and (h) gradient 3-D fast-marching methods [45].

A Bayesian level set approach was proposed for a semi-automatic segmentation of the lumen, intima, and media borders using the shifted Rayleigh law as a model for the gray level statistics [45]. This work is based on the previously published Bayesian level set method of Sifakis [51]. Robustness to initialization was assessed, and a comparison made to an intensity

gradient level-set method, intensity gradient based snakes [48] and PDF snakes. Fifteen IVUS images were used, acquired at 20 Mhz without ECG-gating, and with three different initializations. The PDF-snakes were more stable on average.

Recently, two approaches have been published which aim to incorporate high-level knowledge in IVUS image segmentation. A machine learning approach mimicking the human visual system was proposed for automatic detection of the luminal and the medial-adventitial borders in [52]. The accuracy of the method was assessed on a reasonable data set. Bovenkamp [53], considered solving the segmentation problem using a multiagent knowledge approach. Its elaborate high-level knowledge (450 rules) takes control over simple low-level segmentation algorithm.

A major drawback of IVUS is its inability to consider the vessel curvature and the orientation of the imaging catheter. Hence, quantifications performed on these data are inevitably distorted, since the vessel curvature remains unconsidered. Fusion between intravascular ultrasound and biplane angiography provides a solution for correct 3-D reconstruction of the IVUS data (see, e.g., [54] and [55]).

### 3.5 Obstetrics and Gynecology

Ultrasound measurements play a significant role in obstetrics as an accurate means for the estimation of the fetal age. Several parameters are used as aging parameters, the most important of which are the biparietal diameter (BPD), occipito-frontal diameter (OFD), head circumference (HC) and femur length (FL) [56]. Serial measurement of these parameters over time is used to determine the fetal condition. Thus, consistency and reproducibility of measurements is an important issue.

The noninvasive nature of ultrasound is a strong argument for its use in obstetrics and gynecology. In obstetrics, segmentation provides valuable measurements in order to assess the growth of the fetus and in diagnosis of fetal malformation. Most analysis is based on 2-D scans.

Muzzolini[57] used a split-and merge segmentation approach to segment 2-D ultrasound images of ovarian follicles. The split and merge operations were controlled by means of a simulated annealing algorithm (Metropolis). The authors used a texture-based measure for block comparison in the splitting and merging process which takes into account the block size. In a later work, the same team proposed a robust texture feature selection method based on outlier rejection to be used in the segmentation algorithm [58].

A semi-automatic method for ovarian follicles segmentation was reported by Sarty [59]. The technique is a knowledge based approach and is similar to earlier work of the team [46]. It simultaneously detects the inner and the outer border of the follicle of interest, which was interactively selected by defining an angular region of interest. Both border detections were based on the minimization of a cost function using heuristic graph searching techniques. Polar coordinates were used and edges strength and direction were considered in the cost function definition which incorporates some prior knowledge. The outer wall was automatically detected after the detection of the inner wall, for which frequent manual correction were required.

The binary segmentation algorithm was demonstrated on ultrasound images with ovarian cysts in [61] and was used in the segmentation step in a recent work for quantitative analysis

and malignancy detection of ovarian masses [62]. The demonstration of the normality of the local entropy under more complete models, like the generalized K-distribution, is still to be done.

All of the above methods operate in 2-D which mimics clinical practice. However, one is really looking at a 3-D object, and the interest is to measure volume rather than a linear dimension (Euclidean distance). Romeny [63] described a method for segmenting follicles from 3-D ultrasound data which was fully automatic and consisted of two steps (follicles centers detection followed by 1-D edge detection along radial rays generated from the follicle's center). The centers detection method was based on the so-called winding number of the intensity singularity. The edge points along the 1-D profiles were detected using a robust multiscale zero-crossing of the second derivative. The lifetime of an edge pattern over scale was used as a measure of its significance.

Fig.4. Shows an example of fetal head detection for finding the weight

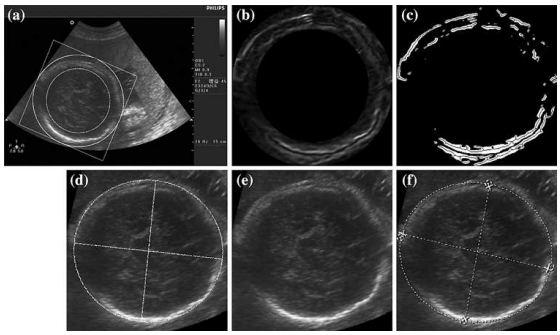


**Figure 4.** Segmentation and measurement of fetal head. (a) ROI definition, (b) Edge map detected by the ICOV, (c) Salient edges map with its skeleton, (d) Head contour extracted by program, (e) Original image, (f) Manually extracted head contour[a]

## 4. Classification of Ultrasound Segmentation based on Methods Applied

Due to the relatively low quality of clinical ultrasound images, a good ultrasound image segmentation method needs to make use of all task-specific constraints or priors.

### 4.1 Speckle Noise or Features

Traditionally, speckles in an ultrasound image were treated as noise and algorithms were proposed to reduce them. More recent studies used speckles to measure tissue displacement and optimize image registration. Speckle gives ultrasound images their characteristic granular appearance. It inherently exists in coherent imaging, including ultrasound imaging.

The received echo signals are obtained by a coherent summation of echo signals from many ultrasound scatterers. Speckle has a random and deterministic nature as it is formed from backscattered echoes of randomly or coherently distributed scatterers in the tissue [64], [65]. It has been shown that the statistical properties of the received signal, and thus of the echo envelope, depend on the density and the spatial distribution of the scatters [64]. Several distribution families have been proposed in the literature. For the special case of a large number of randomly located scatterers, the statistics of the envelope signal shows a Rayleigh distribution (see e.g., [64] and [65]). In this condition, the speckle is called fully developed. Deviations from such special scattering conditions have been previously modeled via

• The Rice distribution to account for a coherent component due to the presence of a regular structure of scatterers within the tissue [64].

• The K-distribution to account for low effective scatter density (partially developed speckle)

Unfortunately, the Rician family fails to account for reduced scatterer densities, and the - distribution model does not take into account the presence of a coherent component. General models have been proposed in the literature namely the generalized K-distribution and the homodyned K-distribution and most recently the Rician Inverse of Gaussian distribution [66]. The three models are general and can account for the different scattering conditions. However, the analytical complexity with these families is significant. Some effort has been put into efficiently estimating the parameters [67] and alternative simple models have also been proposed such as the Nakagami family.

Fig 5. shows the results of the speckle statistics, where each pixel of AOI is assigned the value calculated from the ridge tree at which the pixel's outgoing stream ends[71].

There is also an extensive literature on speckle reduction which has been proposed as a pre-segmentation step; recent works include wavelets–based methods [68]–[70], anisotropic diffusion methods [72]–[74].

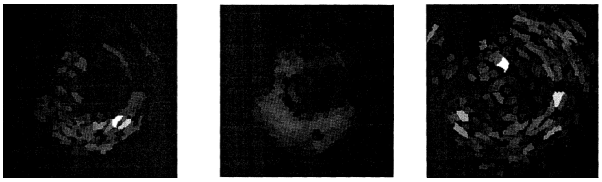

**Figure. 5**(a) Speckle ridge Tree Size (b) Speckle average ridge gray-scale (c) Speckle weighted gray scale

### 4.2 Image Features

In this section we focus on *non-textured* based models including image differencing, histogram analysis, morphology, masking and active contours. Speckle data could be categorised into two groups: *Boundary Speckles*, which represent existing physical boundaries varying in size and distance, and *Random Speckles*, usually smaller in size representing no real object. We have further subdivided this definition within our research, to *Elongated Speckles* (with striated sheath structures) tending to represent tendon internals, and *Dot Speckles* tending to represent tissue (Figure 6(a)).

Klingler et al. [75] presented a semiautomatic technique applying mathematical morphology to segment the endocardium in echocardiograms. A morphological opening filter of radius size 20 was applied to a composite frame (the average of all frames), which removed intensity peaks in the image. The resultant image was then subtracted from the original, retaining edge information partially corrected for greylevel variation, followed by grayscale closing and binary dilation. They extracted a closed contour by iteratively thinning the result, identifying the contour as the inside edge of the endocardium, and proceeded with boundary enhancements. These techniques have been researched in many radiological procedures including elastography [76,77] and angiography [78]. For example, Benkeser et al. [76] used elastography tools to measure tissue displacement under an axial stress and extracted relevant features using binary thresholding and dilation / erosion operators. Figueiredo and Leitao [77] applied a Bayesian framework for estimating a ventricular contour to pre-processed

angiographic images. Images of before and after an injection of a contrast agent were subtracted, removing any occluding osseous structures and leaving only vessels. Bouma et al. [79] also implemented this classic process of calculating a background image and applying morphology and image subtraction for segmenting vessels from intravascular ultrasound images.

J.D. Revella _, M. Mirmehdia and D. McNallyb, "Applied review of ultrasound image feature extraction methods" Initially, they performed image differencing after producing a composite frame from 20 of our sequential images (Figure 6b)). Then the composite and single frames were subtracted, and using a greylevel threshold obtained empirically, and produced a binary image. The output highlighted the tendon edges poorly, but emphasised existing internal sheath regions that could later be used for landmarking experiments (brighter central regions in Figure 6(c)). Next, they created a flat binary matrix defining the neighbourhood of a disk-shaped structured element with radius 4. They used a disk-shape as a result of our earlier definition of *Dot Speckle* characteristics (Klinger et al. [75] used a hexagon structure sometimes leading to errors). Then performed morphological opening by eroding the composite frame with our disk structure to remove, by iterative reduction, hyperechoic *Dot Speckle* intensity regions, and applied a final binary dilation for restoration. To extract the final contour we iteratively thinned the image giving comparable results to [75], but failed to accurately extract tendon features for use in their application (Figure 6(d)). Additionally, we extended our analysis by applying anisotropic diffusion [81] with 10 iterations as shown in Figure 6(e) that proved effective for smoothing speckle regions while preserving and enhancing the contrast at sharp intensity gradients. Figure 6(f) shows much better edge features from applying iterative thinning to the thresholded diffusion output, with longitudinal lines displaying the approximate outside edges of the tendon.

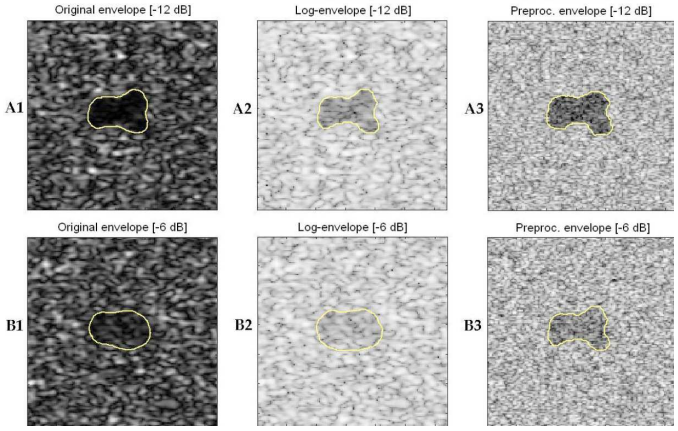


**Figure. 6**(a) Hand labelled original ROI: Pulmarus Longus Tendon (PLT) dotted boundary and Elongated Speckle (ES) and Dot Speckle (DS) regions, (b) composite frame, (c) image subtraction (Frame 1 Motion), (d) Klingler et al's approach, (e) anisotropic diffusion, (f) final output, after thresholding and thinning of Figure 6(e).

### 4.3 Active Contours

Present study demonstrates that the performance of segmentation algorithms can be substantially improved via applying the latter to *preprocessed* rather than original images. In particular, the proposed method segments ultrasound images in the logarithmic domain, after the images have been subjected to the processes of decorrelation and outlier shrinkage. It is shown that this preprocessing is capable of considerably improving the separability of

segmentation classes, thereby increasing the accuracy of resulting segmentation. The method by means of which the segmentation is performed is based on the technique of *active contours*. [83]The method uses the concept of combining multiple trajectory models in order to track a single target in a randomly distributed cluttered environment [84, 85]. In the previous original work by the authors [86], a PDAF technique was used to extract carotid artery contours from a sequence of ultrasound images in real-time. In the current work, we combine the PDAF technique with the IMM estimator in order to increase the accuracy of the extracted contours. This combination has been necessary, since in contrast to the carotid artery that has a well-defined circular shape, prostate boundary can have almost any arbitrary shape and come in different sizes. Because of the low computational cost of the algorithm, it has a great potential to be implemented for real-time applications.

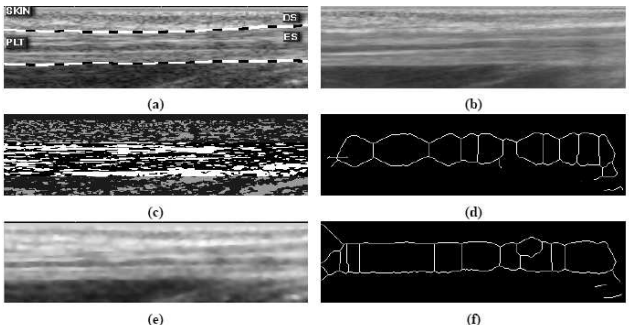


**Figure 7.** (A1-A3) Segmentation of the original, log-, and preprocessed envelopes at -12 dB constrast; (B1-B3) Segmentation of the original, log-, and preprocessed envelopes at -6 dB constrast[82].

### 4.4 B-Spline

A snake is a curve that evolves from an initial position towards the boundary of an object, minimizing some energy functional [87, 88, 90]. Such functional consists of two terms: the internal energy and the external energy. The first term affects the smoothness of the curve,

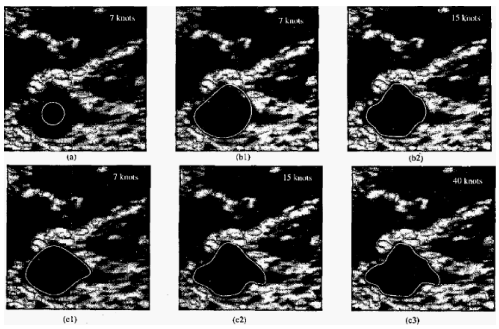


**Figure 8**. Result of the proposed B-spline snake segmentation for different number of knots and parameters [97]

while the second attracts the snake towards image features. Splines can be effectively integrated in the snakes model, as they can characterize a continuous parametric curve by a vector of control points [89]. The benefit of using splines comes from the implicit properties

of the model, including the local support and the control of the continuity of the curve. The functional defining the energy of a B-spline having the equation *s(u) = (x(u), y(u))* is [87]:

*E*snake = *E*intern*(s(u))* + *E*extern*(s(u))*

## 5. Conclusions

Here we discussed the formation of Ultrasound Images and there advantages in medical field. Because of increasing applications in the field of ultrasound images in diagnosis as well as therapeutic purposes we need to enhance the feature which we require for further processing. There are different techniques for doing this. One of these is segmentation which is a wide area of image processing. So in the other section we briefly discussed the segmentation methods.

After getting the idea about segmentation and ultrasound images we discussed different techniques and papers on the basis of particular clinical application as well as on the basis of methods used to segment out the ultrasound images.

## 6. References

[1] J A Noble "Ultrasound image segmentation and tissue characterization" Part H: J. Engineering in Medicine, Vol. 223, PP. 1-10, June 2009.

[2] Hill, C. R., Bamber, J. C., and ter Haar, G. R. "Physical principles of medical ultrasonics", 2nd edition, 2004 (John Wiley, Chichester, UK).

[3] J.M.B. Dias and J.M.N. Leitao. "Wall position and thickness estimation from sequences of echocardiographic" images. IEEE T. Med. Imag., 15:25–38, 1996.

[4] I. Mikic, S. Krucinski, and J.D. Thomas. "Segmentation and tracking in echocardiographic sequences: active contours guided by optical flow estimates" IEEE T. Med. Imag., 17:274–284, 1998.

[5] A. Mojsilovic, M.V. Popovic, A.N. Neskovic, and A.D. Popovicq. "Wavelet image extension foranalysis and classifcation of infarcted myocardial tissue", IEEE T. Biomed. Eng., 44:856–866, 1997.

[6] Y. Zimmerand R. Tepper and S. Akselrod. A two-dimensional extension of minimum cross entropy thresholding for the segmentation of ultrasound images. Ultrasound Med. Biol., 22:1183–1190, 1996

[7] G. Coppini, R. Poli, and G. Valli. Recovery of the 3-D shape of the left ventricle from echocardiographic images. IEEE T. Med. Imag., 14:301–317, 1995.

[8] T.N. Jones and D.N. Metaxas. Segmentation using deformable models with affinity-based localization. Lecture Notes in Computer Science, 1205:53–52, 1997.

[9] D. Kucera and R.W. Martin. Segmentation of sequences of echocardiographic images using a simplified 3D active contour model with region based external forces. Comput. Med. Im. Graph., 21:1–21, 1997.

[10] F. Lefebvre, G.Berger, and P. Laugier. Automatic detection of the boundary of the calcaneus from ultrasound parametric images using an active contour model: clinical assessment. IEEE T. Med. Imag., 17:45–52, 1998.

[11] S.D. Pathak, P.D. Grimm, V. Chalana, and Y. Kim. Pubic arch detection in transrectal ultrasound guided prostate cancer therapy. IEEE T. Med. Imag., 17:762–771, 1998.

[12] S.D. Pathak, V.Chalana, and Y.M. Kim. Interactive automatic fetal head measurements from ultrasound images using multimedia computer technology. Ultrasound in Medicine and Biology, 23:665–673, 1997.

[13] M. Sonka, X. Zhang, M. Siebes, M.S. Bissing, S.C. DeJong, S.M Collins, and C.R. McKay. Segmentation of intravascular ultrasound images: a knowledge-based approach. IEEE T. Med. Imag., 14:719–732, 1995.

[14] A. Yezzi, S. Kichenassamy, A. Kumar, P. Olver, and A. Tannenbaum. A geometric snake model for segmentation of medical imagery. IEEE T. Med. Imag., 16:199–209, 1997.

[15] J. Dias and J. Leitão, "Wall position and thickness estimation from sequences of echocardiograms images," IEEE Trans. Med. Imag., vol. 15, no. 1, pp. 25–38, Jan. 1996.

[16] I. Mikic, S. Krucinski, and J. D. Thomas, "Segmentation and tracking in echocardiographic sequences: Active contours guided by optical flow estimates," IEEE Trans. Med. Imag., vol. 17, no. 2, pp. 274–284, Apr. 1998.

[17] J. G. Bosch, S. C. Mitchell, B. P. F. Lelieveldt, F. Nijland, O. Kamp, M. Sonka, and J. H. C. Reiber, "Automatic segmentation of echocardiographic sequences by active appearance motion models," IEEE Trans. Med. Imag., vol. 21, no. 11, pp. 1374–1383, Nov. 2002.

[17] O. T. von Ramm and S. W. Smith, “Real time volumetric ultrasound imaging system,” J. Digit. Imag., vol. 3, no. 4, pp. 261–266, Nov. 1990.

[18] T. Binder, “Three-dimensional echocardiography—Principles and promises,” J. Clin. Basic Cardiol., vol. 5, no. 2, pp. 149–152, 2002. 11 Hill, C. R., Bamber, J. C., and ter Haar, G. R. Physical principles of medical ultrasonics, 2nd edition, 2004 (John Wiley, Chichester, UK).

[19] A. Mishra, P. K. Dutta, and M. K. Ghosh, “A GA based approach for boundary detection of left ventricle with echocardiographic image sequences,” Image Vis. Comput., vol. 21, pp. 967–976, 2003.

[20] M. Mignotte and J. Meunier, “A multiscale optimization approach for the dynamic contour-based boundary detection issue,” Comput. Med. Imag. Graph., vol. 25, no. 3, pp. 265–275, May–Jun. 2001.

[21] J. Y. Yan and T. Zhuang, “Applying improved fast marching method to endocardial boundary detection in echocardiographic images,” Pattern Recognit. Lett., vol. 24, no. 15, pp. 2777–2784, Nov. 2003.

[22] O. Husby and H. Rue, “Estimating blood vessel areas in ultrasound images using a deformable template model,” Statist. Model., vol. 4, no.3, pp. 211–226, 2004.

[24] M. Franke and H. P. Kohl, “Second-generation real-time 3-D echocardiography: A revolutionary new technology,” Medicamundi, vol. 47, no. 2, p. 3440, 2003.

[25] Y. Chen, F. Huang, H. D. Tagare, M. Rao, D.Wilson, and E. A. Geiser, “A coupled minimization problem for medical image segmentation with priors,” Int. J. Comput. Vis., to be published.

[26] A. Stavos, D. Thickman, C. Rapp, M. Dennis, S. Parker, and S. G. A., “Solid breast modules: Use of sonography to distinguish between benign and malignant lesions,” Radiology, vol. 196, pp. 123–134, 1995.

[27] V. Jackson, “Management of solid breast modules: What is the role of sonography?,” Radiology, vol. 196, pp. 14–15, 1995.

[28] P. Arger,C. Sehgal, E. Conant, J. Zuckerman, S. Rowling, and J. Patton, “Interreader variability and predictive value of is descriptions of solid masses: Pilot study,” Acad. Radiol., vol. 8, pp. 335–342, 2001.

[29] K. Horsch, M. L. Giger, L. A. Venta, and C. J. Vyborny, “Automatic segmentation of breast lesions on ultrasound,” Med. Phys., vol. 28, no. 8, pp. 1652–1659, Aug. 2001.

[30] D. R. Chen, R. F. Chang, W. J. Kuo, M. C. Chen, and Y. L. Huang, “Diagnosis of breast tumors with sonographic texture analysis using wavelet transform and neural networks,” Ultrasound Med. Biol., vol. 28, no. 10, pp. 1301–1310, Oct. 2002.

[31] G. F. Xiao, M. Brady, J. A. Noble, and Y. Y. Zhang, “Segmentation of ultrasound B-mode images with intensity inhomogeneity correction,” IEEE Trans. Med. Imag., vol. 21, no. 1, pp. 48–57, Jan. 2002.

[32] D. Boukerroui, A. Baskurt, J. A. Noble, and O. Basset, “Segmentation of ultrasound images multiresolution 2-D and 3-D algorithm based on global and local statistics,” Pattern Recognit. Lett., vol. 24, no. 4–5, pp. 779–790, Feb. 2003.

[33] A. Madabhushi and D. N. Metaxas, “Combining low-, high-level and empirical domain knowledge for automated segmentation of ultrasonic breast lesions,” IEEE Trans. Med. Imag., vol. 22, no. 2, pp. 155–169, Feb. 2003.

[34] B. Sahiner, H. P. Chan, M. A. Roubidoux, M. A. Helvie, L. M. Hadjiiski, A. Ramachandran, C. Paramagul, G. L. LeCarpentier, A. Nees, and C. Blane, “Computerized characterization of breast masses on three dimensional ultrasound volumes,” Med. Phys., vol. 31, no. 4, pp. 744–754, Apr. 2004.

[35] L. X. Gong, S. D. Pathak, D. R. Haynor, P. S. Cho, and Y. Kim, “Parametric shape modeling using deformable superellipses for prostate segmentation,” IEEE Trans. Med. Imag., vol. 23, no. 3, pp. 340 349, Mar. 2004.

[36] C. Knoll, M. Alcaniz, V. Grau, C. Monserrat, and M. Carmen Juan, “Outlining of the prostate using snakes with shape restrictions based on the wavelet transform,” Pattern Recognit., vol. 32, no. 10, pp. 1767–1781, Oct. 1999.

[37] P. Abolmaesumi and M. R. Sirouspour, “An interacting multiple model probabilistic data association filter for cavity boundary extraction from ultrasound images,” IEEE Trans. Med. Imag., vol. 23, no. 6, pp. 772–784, Jun. 2004.

[38] Y. Yu, J. A. Molloy, and S. T. Acton, “Segmentation of the prostate from suprapubic ultrasound images,” Med. Phys., vol. 31, no. 12, pp. 3474–3484, Dec. 2004.

[39] Y. Yu and S. T. Acton, “Speckle reducing anisotropic diffusion,” IEEE Trans. Image Process., vol. 11, no. 11, pp. 1260–1270, Nov. 2002.

[40] ——, “Edge detection in ultrasound imagery using instantaneous coefficient of variation,” IEEE Trans. Image Process., vol. 13, no. 12, pp. 1640–1655, Dec. 2004.

[41] B. Levienaise-Obadia and A. Gee, “Adaptive segmentation of ultrasound images,” Image Vis. Comput., vol. 17, no. 8, pp. 583–588, Jun. 1999.

[42] M. Martin-Fernandez and C. Alberola-Lopez, “An approach for contour detection of human kidneys from ultrasound images using Markov random fields and active contours,” Med. Image Anal., vol. 9, pp. 1–23, 2005.

[43] Z. Dokur and T. Ölmez, “Segmentation of ultrasound images by using a hybrid neural network,” Pattern Recognit. Lett., vol. 23, no. 14, pp. 1825–1836, Dec. 2002.

[44] C. Kotropoulos and I. Pitas, “Segmentation of ultrasonic images using support vector machines,” Pattern Recognit. Lett., vol. 24, no. 4–5, pp. 715–727, Feb. 2003.

[45] M.-H. R. Cardinal, J. Meunier, G. Soulez, E. Thrasse, and G. Cloutier, “Intravascular ultrasound image segmentation: A fastmarching method,” in Medical Image Computing and Computer Assisted Intervention, ser. Lect. Note Comput. Sci. Berlin: Springer-Verlag, 2003, pp. 432–439.

[46] M. Sonka, X. M. Zhang, M. Siebes, M. S. Bissing, S. C. DeJong, S. M. Collins, and C. R. McKay, “Segmentation of intravascular ultrasound images: A knowledge-based approach,” IEEE Trans. Med. Imag., vol. 14, no. 4, pp. 719–732, Dec. 1995.

[47] R. Shekhar, R. M. Cothren, D. G. Vince, S. Chandra, J. D. Thomas, and J. F. Cornhill, “Three dimensional segmentation of luminal and adventitial borders in serial intravascular ultrasound images,” Comput. Med. Imag. Graph., vol. 23, pp. 299–309, Dec. 1999.

[48] J. D. Klingensmith, R. Shekhar, and D. G. Vince, “Evaluation of three dimensional segmentation algorithms for the identification of luminal and medial-adventitial borders in intravascular ultrasound images,” IEEE Trans. Med. Imag., vol. 19, no. 10, pp. 996–1011, Oct. 2000.

[49] E. Brusseau, C. L. de Korte, F. Mastik, J. Schaar, and A. F. W. van der Steen, “Fully automatic luminal contour segmentation in intracoronary ultrasound imaging—A statistical approach,” IEEE Trans. Med. Imag., vol. 23, no. 5, pp. 554–566, May 2004.

[50] X. M. Pardo, P. Radeva, and D. Cabello, “Discriminant snakes for 3-D reconstruction of anatomical organs,” Med. Image Anal., vol. 7, no. 3, pp. 293–310, Sep. 2003.

[51] E. Sifakis, C. Garcia, and G. Tziritas, “Bayesian level sets for image segmentation,” J. Visual Commun. Image Representation, vol. 13, no. 1–2, pp. 44–64, Mar. 2002.

[52] M. E. Olszewski, A.Wahle, S. C. Mitchell, and M. Sonka, “Segmentation of intravascular ultrasound images: A machine learning approach mimicking human vision,” in Int. Congress Series, Jun. 2004, vol. 1268, pp. 1045–1049.

[53] E. G. P. Bovenkamp, J. Dijkstra, J. G. Bosch, and J. H. C. Reiber, “Multi-agent segmentation of IVUS images,” Pattern Recognit., vol. 37, no. 4, pp. 647–663, Apr. 2004.

[54] P. Radeva, , J. S. Suri and S. Laxminarayan, Eds., Angiography and plaque imaging: Advanced segmentation techniques. Boca Raton, FL: CRC, 2003, pp. 397–450.

[55] A. Wahle, S. C. Mitchell, R. M. Long, and M. Sonka, “Accurate volumetric quantification of coronary lesions by fusion between intravascular ultrasound and biplane angiography,” Comput. Assist. Radiol. Surg., vol. 1214, pp. 549–554, 2000.

[56]. R. Sanders and A. James, The Principles and Practice of Ultrasonorrraphy in Obstetrics and Gynecology, 3rd edition, Appleton-Century-Crofts, Connecticut, 1985, Ch. 9 & 10.

[57] R. Muzzolini, Y. H. Yang, and R. Pierson, “Multiresolution texture segmentation with application to diagnostic ultrasound images,” IEEE Trans. Med. Imag., vol. 12, no. 1, pp. 108–123, Mar. 1993.

[58] ——, “Texture characterization using robust statistics,” Pattern Recognit., vol. 27, no. 1, pp. 119–134, Jan. 1994.

[59] G. E. Sarty, W. D. Liang, M. Sonka, and R. A. Pierson, “Semiautomated segmentation of ovarian follicular ultrasound images using a knowledge-based algorithm,” Ultrasound Med. Biol., vol. 24, no. 1, pp.27–42, Jan. 1998.

[60] A. Krivanek and M. Sonka, “Ovarian ultrasound image analysis: Follicle segmentation,” IEEE Trans. Med. Imag., vol. 17, no. 6, pp.935–944, Dec. 1998.

[61] Y. Zimmer, R. Tepper, and S. Akselrod, “A two-dimensional extension of minimum cross entropy thresholding for the segmentation of ultrasound images,” Ultrasound Med. Biol., vol. 22, no. 9, pp. 1183 1190, 1996.

[62] Y. Zimmer, S. Tepper, and R. Akselrod, “An automatic approach for morphological analysis and malignancy evaluation of ovarian masses using B-scans,” Ultrasound Med. Biol., vol. 29, no. 11, pp. 1561–1570, 2003.

[63] B. M. T. Romeny, B. Titulaer, S. Kalitzin, F. Scheffer, G. Broekmans, J. Staal, and E. T. Velde, "Computer assisted human follicle analysis for fertility prospects with 3-D ultrasound," in Info. Process. in Med. Imaging, ser. Lect. Note Comput. Sci. Berlin, Germany: Springer-Verlag, 1999, vol. 1613, pp. 56–69.

[64] R. F. Wagner, S. W. Smith, J. M. Sandrik, and H. Lopez, "Statistics of speckle in ultrasound B scans," IEEE Trans. Sonics Ultrason., vol. 30, no. 3, pp. 156–163, 1983.

[65] C. B. Burckhardt, "Speckle in ultrasound B-mode scans," IEEE Trans. Sonics Ultrason., vol. SU-25, no. 1, pp. 1–6, 1978.

[66] T. Eltoft, "Speckle: Modeling and filtering," in Norwegian Signal Process. Symp., Bergen, Norway, Oct. 2–3, 2003 [Online]. Available: http://www.norsig.no/norsig2003/

[67] V. Dutt and J. F. Greenleaf, "Speckle analysis using signal to noise ratios based on fractional order moments," Ultrason. Imag., vol. 17, no. 4, pp. 251–268, Oct. 1995.

[68] A. Achim, A. Bezerianos, and T. P. , "Novel Bayesian multiscale method for speckle removal in medical ultrasound images," IEEE Trans. Med. Imag., vol. 20, no. 8, pp. 772–783, Aug. 2001.

[200] S. Gupta, R. C. Chauhan, and S. C. Sexana, "Wavelet-based statistical approach for speckle reduction in medical ultrasound images," MBEC, vol. 42, pp. 189–192, 2004.

[69] X. Zong, A. F. Laine, and E. A. Geiser, "Speckle reduction and contrast enhancement of echocardiograms via multiscale nonlinear processing," IEEE Trans. Med. Imag., vol. 17, no. 4, pp. 532–540, Aug. 1998.

[70] C.-Y. Xiao, S. Zhang, and Y.-Z. Chen, "A diffusion stick method for speckle suppression in ultrasonic images," Pattern Recognit. Lett., vol. 25, no. 16, pp. 1867–1877, Dec. 2004.

[71] Dongbai Guo, "Intravascular Ultrasound Speckle Statistics", IEEE Engineering in Medicine and Biology Society, Vol. 20, No 2,1998.

[72] K. Z. Abd-Elmoniem, A.-B. M. Youssef, and Y. M. Kadah, "Realtime speckle reduction and coherence enhancement in ultrasound imaging via nonlinear anisotropic diffusion," IEEE Trans. Biomed. Eng., vol. 49, no. 9, pp. 997–1014, Sep. 2002.

[73] K. Krissian, K. Vosburgh, R. Kikinis, and C.-F. Westin, Anistropic diffusion of ultrasound constrained by speckle noise model Lab. Math. Imaging, Harvard Medical School, Cambridge, MA, 2004, Tech. Rep.

[74] C. Tauber, H. Batatia, and A. Ayache, "A robust speckle reducing anisotropic diffusion," in IEEE Int. Conf. Image Process., Singapore, 2004, vol. 1, pp. 247–250.

[75] J.Klingler, J. Vaughan, T. Fraker et al. "Segmentation of echocardiographic images using mathematical morphology." IEEE Trans. on Biomedical Engineering 35, pp. 925–934, 1988.

[76] E. Konofagou & J. Ophir. "A new elastographic method for estimation and imaging of lateral displacements, lateral strains, corrected axial strains and poisson's ratios in tissues." Ultrasound in Medicine & Biology 24, pp. 1183–1199, 1998.

[77] P. Benkeser, J. Jackson & F. Nichols. "3d ultrasonic imaging of the structure and elasticity of the carotid bifurcation." Proc. IEEE Ultrasonics Symposium pp. 1419–1422, 1995.

[78] M. de Figueiredo & J. Leitao. "Bayesian estimation of ventricular contours in angiographic images." IEEE Trans. On Medical Imaging 11, pp. 416–429, 1992.

[79] C. J. Bouma, K. J. Zuiderveld & M. A. Viergever. "Quantitative evaluation of (semi)-automated segmentation of intravascular ultrasound subtraction images." In Abstracts of the 11th Symposium on Echocardiology. 1995.

[80] P. Perona & J. Malik. "Scale-space and edge detection using anisotropic diffusion." IEEE-PAMI 12, pp. 629–639, 1990.

[81] Y. L. Huang and D. R. Chen, "Watershed segmentation for breast tumor in 2-D sonography," Ultrasound Med. Biol., vol. 30, no. 5, pp. 625–632, May 2004.

[82]Oleg Michailovich, Allen Tannenbaum,"segmentation of medical ultrasound images using active contours", IEEE V - 513 ICIP 2007.

[83]P. Abolmaesumi, M.R. Sirouspour," segmentation of prostate contours from ultrasound images", proc IEEE, ICASSP,pp.517-520, 2004.

[84] Y. Bar-Shalom and T.E. Fortmann, Tracking and Data Association, Academic Press Inc., 1988.

[85] T. Kirburajan, Y. Bar-Shalom, W.D. Blair, and G.A. Watson, "IMMPDAF for radar management and tracking benchmark with ECM," IEEE Trans. Aerospace and Electronic Systems, vol. 34, no. 4, pp. 1115–1134, 1998.

[86] P. Abolmaesumi, S.E. Salcudean, W.H. Zhu, M.R. Sirouspour, and S.P. DiMaio, "Image-guided control of a robot for medical ultrasound," IEEE Trans. Robot. Autom., February 2002.

[87] Cohen, L. (1991). On active contour models and balloons. Computer Vision, Graphics, And Image Processing: Image nderstanding, 53, 211–218.

[88] Kass, M., Witkin, A., & Terzopoulos, D. (1988). Snakes: Active contour models. International Journal of Computer Vision, 1, 321–332.

[89] Precioso, F., Barlaud, M., Blu, T., & Unser, M. (2003). Smoothing b-spline active contour for fast and robust image and video segmentation. Image Processing, 2003. Proceedings. 2003 International Conference on (Vol. 1, pp. 37–40).

[90] Xu, C., Prince, J. L. (1998). Snakes, shapes, and gradient vector flow. IEEE Transactions on Image Processing, 7, 359–369.

[91] Rong Lu, Yi Shenl, Qiang Wang, "Edge Detection Based on Early Vision Model Incorporating Imiproved Directional Median Filtering," IEEE instrumentation and measurement technology conerence (aII2004), pp. 441-443, 2004

[92] Chung-Ming Chen, Henry Horng-Shing Lu. Ko-Chung Han, "A textural approach based on gabor functions for texture edge detection in ultrasounld images," ULtrasound in AMed & Biol., Vol. 27. No. 4, pp. 515-534, 2001.

[93] G. Jacob, J. A. Noble, A. D. Kelion, and A. P. Banning, "Quantitative regional analysis of myocardial wall motion," Ultrasound Med. Biol., vol. 27, no. 6, pp. 773–784, 2001.

[94] G. Jacob, J. A. Noble, C. Behrenbruch, A. D. Kelion, and A. P. Banning, "A shape-space-based approach to tracking myocardial borders and quantifying regional left-ventricular function applied in echocardiography," IEEE Trans. Med. Imag., vol. 21, no. 3, pp. 226–238, Mar.

2002.

[95] S. C. Mitchell, J. G. Bosch, B. P. F. Lelieveldt, R. J. van der Geest, J. H. C. Reiber, and M. Sonka, "3-D active appearance models: Segmentation of cardiac MR and ultrasound images," IEEE Trans. Med. Imag., vol. 21, no. 9, pp. 1167–1178, Sep. 2002.

[96] S. Malassiotis and M. G. Strintzis, "Tracking the left ventricle in echocardiographic images by learning heart dynamics," IEEE Trans. Med. Imag., vol. 18, no. 3, pp. 282–290, Mar. 1999.

[97 ] Clovis Tauber , Hadj Batatia, Alain Ayache, "Robust B-Spline Snakes for Ultrasound Image Segmentation", Springer Science ,Business Media, LLC., 2008.

[98]Haihua Liu1, 2, Changsheng Xie and Zhouhui Chen and Yi Lei, "Segmentation of Ultrasound Image Based on Morphological Operation and Fuzzy Clustering" Breast Cancer Research and Treatment, pp-179–185,2005

biography. Personal hobbies will be deleted from the biography.

## Authors

**Kalpana Saini** graduated in Electrical and Electronics from college of Engg. Roorkee India, in 2006 and received her Master's Degree in Instrumentation and Control Engg.from Dr. B.R. Ambedkar N.I.T. Jalandhar, Punjab, India in 2009. Currently she is a Research Scholar with ISP academic group of Department of Electrical Engg at IIT Roorkee, India. She has published a no. of Research papers in Journals and Conferences. Her current Research Interests include Image Processing with Echo Images.

**Dr ML Dewal** He did his B.Tech in Electrical Engg. in 1972 from G.B. Pant University of Agriculture and Technology, Pantnagar, USNagar, India. He did his M.E. (PSE) and Ph.D. in Electrical Engineering both from IIT, Roorkee, erstwhile University of Roorkee in the year 1974 and 1982, respectively. Currently he is working as Assistant Professor In IIT Roorkee. His areas of Interest are Power System Protection and Digital Image Processing.

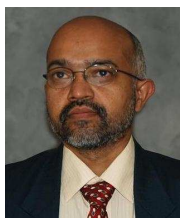

**Dr.Manojkumar Rohit** has done his M.B.B.S. from Jawaharlal Institute of Post Graduate Medical Education & Research-Pondicherry in Aprial 1992. After that he has done M.D. from AIIMS Delhi in May 1996. He has worked as Senoir Resident in AIIMS during Oct 1996-March 1998 and as a

D.M.(Cardiology) in PGIMER Chandigarh upto May 2000. Currently he is working as an Associate Professor in Cardiology Deptt in PGIMER Chandigarh since july 2007.